Computers & Geosciences 34 (2008) 1769–1780

Contents lists available at ScienceDirect

Computers & Geosciences

journal homepage: www.elsevier.com/locate/cageo

An Excel spreadsheet to recast analyses of garnet into end-member components, and a synopsis of the crystal chemistry of natural silicate garnets ☆

Andrew J. Locock *

Department of Earth and Atmospheric Sciences, University of Alberta, 1-26 Earth Sciences Building, Edmonton, Alberta, Canada T6G 2E3

ARTICLE INFO

Article history:
Received 17 April 2007
Received in revised form
11 November 2007
Accepted 30 December 2007

Keywords:
Crystal chemistry
Electron microprobe
End-members
Excel
Garnet
Spreadsheet

ABSTRACT

A Microsoft Excel spreadsheet has been programmed that allows users to calculate with ease the molar proportions of garnet end-members from chemical analyses. Recent advances in the understanding of the crystal chemistry of natural garnets, especially of the Ti-bearing garnets, are used to evaluate 29 end-members (15 species and 14 hypothetical end-members) for each analysis. The amounts of Fe^{2+} and Fe^{3+} (and Mn^{3+}, if necessary) are calculated by stoichiometric constraints if these quantities have not been measured. The input data can include: SiO_2, TiO_2, ZrO_2, SnO_2, Y_2O_3, Al_2O_3, Sc_2O_3, Cr_2O_3, V_2O_3, FeO, Fe_2O_3, MnO, MgO, CaO, Na_2O, H_2O+ and F. The spreadsheet can be used with large data sets (up to 100 analyses at a time), and is accompanied by results calculated for 470 garnet analyses taken from the literature. The spreadsheet employs a simple scoring algorithm to measure the quality of a garnet analysis. The propagation of error from the input chemical data to the calculation of end-member proportions is also discussed briefly.

1. Introduction

Natural garnets are an important group of orthosilicate minerals that occur in a wide variety of geologic environments (Deer et al., 1997), and whose chemical compositions are of particular significance in geothermobarometry (e.g., Spear, 1993). The general formula of anhydrous garnet may be expressed as $\{X_3\}[Y_2](Z_3)\phi_{12}$, where *X*, *Y* and *Z* are cations, { } indicates eightfold coordination of the cations, [ ] denotes octahedral coordination, ( ) signifies tetrahedral coordination and ϕ corresponds to the anion site. The garnet crystal structure has been described as one of considerable chemical compliance (Hawthorne, 1981): it can accommodate a wide variety of elements, with the result that a large number of synthetic compounds adopt this structure type (Geller, 1967; Hawthorne, 1981). In natural systems, specimens of garnet exhibit extensive solid solution; consequently, their chemical compositions are often expressed in terms of the molar proportions of end-member components (Hawthorne, 2002). Although there are 15 cubic mineral species in the garnet group (Mandarino and Back, 2004), the chemical compositions of natural garnets commonly cannot be fully expressed in terms of these species. Hypothetical end-members (those end-members that have not been shown to form individually a majority of any natural garnet specimen, and thus do not warrant the status of mineral species) are also required to describe the chemical complexity inherent in many natural specimens of garnet.

Several procedures have been presented for the recalculation of analyses of garnet into molar proportions of end-member components. Rickwood (1968) presented a thorough discussion of the difficulties inherent in recasting garnet analyses, including a discussion of which end-members are appropriate and the influence of the

☆ Code available from server at http://www.iamg.org/CGEditor/index.htm.

* Tel.: +1 780 492 2518; fax: +1 780 492 2030.
E-mail address: alocock@ualberta.ca

0098-3004/$ - see front matter © 2008 Elsevier Ltd. All rights reserved.
doi:10.1016/j.cageo.2007.12.013

calculation sequence upon the results. The recursive procedure of Rickwood (1968), which uses 19 end-members, was programmed into an early mainframe computer and is the foundation of the BASIC program of Knowles (1987), the Lotus 1-2-3 spreadsheet of Friberg (1989) and the linear programming method of Yang (1991). Although Rickwood's procedure has been widely used (cf. the compilation of Deer et al., 1997), it was criticized by Muhling and Griffin (1991), largely on the basis of its inappropriate treatment of titanium. The latter authors presented a QuickBASIC program that makes use of 16 end-members, and which produces results that differ from those of Rickwood (1968), most notably in the treatment of chromium, iron and titanium.

The Excel spreadsheet described here takes advantage of recent advances in the understanding of the crystal chemistry of natural garnets, especially of the Ti-bearing garnets (Chakhmouradian and McCammon, 2005; Henmi et al., 1995). It is intended to be used with chemical compositional data, rather than with the results of structure refinement or spectroscopic experiments. In order to accommodate the range of major-element compositions observed in nature, 29 possible end-members are evaluated for each analysis (15 mineral species and 14 hypothetical end-members). If the amounts of FeO and Fe_2O_3 have not been measured, stoichiometric constraints are applied to try to achieve charge balance; Mn^{3+} is calculated only for compositions that cannot charge balance with Fe^{3+} alone. Care was taken to ensure that, in so far as is possible, the results are in substantial agreement with those generated by the widely adopted procedure of Rickwood (1968), but with the advantage of a more realistic set of end-members, and the ability to accept a wider range of composition. The spreadsheet can be used with large data sets (up to 100 analyses at a time), and is accompanied by results calculated for 470 garnet analyses from both the recent literature and from Deer et al. (1997). The Microsoft program Excel was selected for this work because of its wide distribution and its ease of use.

2. Crystal chemistry

2.1. Chemical composition

The chemical compositions of natural silicate garnets are dominated by the following elements (listed in order of increasing atomic number): H, O, F, Na, Mg, Al, Si, Ca, Sc, Ti, V, Cr, Mn, Fe, Y, Zr and Sn (Amthauer et al., 1979; Chakhmouradian et al., 2008; Deer et al., 1997; Galuskina et al., 2005). Conventionally, the cations are expressed as oxides in percent by weight. Several other elements are reported only occasionally and only in low concentrations: Li, P, S, Cl, K, Ni, Zn, As, Sr, Nb, Te, Ba, REE, Hf, W and Th. These minor elements are not considered further as they do not normally contribute significantly to the compositions of natural silicate garnets. The non-silicate minerals that are isostructural with the garnet group: berzeliite, $\{Ca_2Na\}[Mg_2](As_3)O_{12}$ (Bubeck and Machatschki, 1935); cryolithionite, $\{Na_3\}[Al_2](Li_3)F_{12}$ (Menzer, 1927); manganberzeliite, $\{Ca_2Na\}[Mn_2](As_3)O_{12}$ (Ito, 1968); palenzonaite, $\{Ca_2Na\}[Mn_2](V_3)O_{12}$ (Basso, 1987); schäferite, $\{Ca_2Na\}[Mg_2](V_3)O_{12}$ (Krause et al., 1999); and yafsoanite, $\{Ca_3\}[Te_2](Zn_3)O_{12}$ (Jarosch and Zemann, 1989) are rare and have not been demonstrated to show extensive solid solution toward the silicate garnets, and are therefore disregarded for the purposes of this work.

2.2. General valence states

The formal valence states of most of the main constituent elements are invariable in the garnet structure: H^+, O^{2-}, F^-, Na^+, Mg^{2+}, Al^{3+}, Si^{4+}, Ca^{2+}, Sc^{3+}, Cr^{3+}, Y^{3+}, Zr^{4+} and Sn^{4+}. However, at least in principle, the first-row transition elements V, Mn, Fe and Ti can adopt two (or more) valence states. In practice, despite the existence of such rare vanadate minerals as palenzonaite, $\{Ca_2Na\}[Mn_2^{2+}](V_3^{5+})O_{12}$ and schäferite, $\{Ca_2Na\}[Mg_2](V_3^{5+})O_{12}$, which have the cubic garnet structure, vanadium in most natural silicate garnets is considered to be present as V^{3+}, as in the mineral species goldmanite, $\{Ca_3\}[V_2](Si_3)O_{12}$, and even when the element is present in only minor or trace quantities (Locock et al., 1995). Similarly, manganese generally occurs as Mn^{2+}, with the exception of highly oxidized compositions in which Mn^{3+} is present, e.g., the garnet-related tetragonal mineral henritermierite, $\{Ca_3\}[Mn_2^{3+}](SiO_4)_2(OH)_4$ (Armbruster et al., 2001). The relative concentrations of Fe^{3+} and Fe^{2+} in garnet can be determined by several methods including classical titrimetry, colorimetry, ^{57}Fe Mössbauer spectroscopy, synchrotron-based X-ray absorption spectroscopy or by calculation from stoichiometric constraints. The topic of the valence state of Ti in garnet is more contentious and is addressed below.

2.3. The valence state of Ti

The major redox couple in natural garnet is the Fe^{3+}–Fe^{2+} pair. Yet, for some natural Ti-rich garnets, the presence of both Ti^{4+} and Ti^{3+} has occasionally been invoked, generally to satisfy the requirement of exact charge balance (and usually without consideration of the effects of propagated analytical uncertainty). The crystal chemistry of Ti-bearing garnets has been carefully evaluated in recent years (Armbruster et al., 1998; Chakhmouradian and McCammon, 2005; Locock et al., 1995), and the existence of Ti^{3+} in natural garnets is not supported by these investigations.

From the perspective of both standard reduction potentials and of geologically relevant oxygen fugacity buffers (cf. Frost, 1991), the reducing conditions required for Ti^{3+}-in-garnet are not likely to occur in terrestrial garnet-forming environments: e.g., the Ti_3O_5–TiO_2 oxygen fugacity buffer is ~4–5 log units below the iron–wüstite buffer at ~1400 K (Ihinger and Stolper, 1986). Although measurement of the intrinsic oxygen fugacities of natural Ti-bearing garnets yielded results close to the iron–wüstite buffer and the iron–quartz–fayalite buffer (Virgo et al., 1976); such types of measurements have been

shown to be less than reliable, based on subsequent investigations and on comparisons with the results of thermodynamic calculations based on heterogeneous mineral equilibria (Luth et al., 1990; Virgo et al., 1988).

Direct experimental evidence of significant amounts of reduced titanium in garnet is lacking. Synthesis of pyrope in the presence of a mixture of Ti_2O_3 and Ti metal has demonstrated that Ti^{3+} can be incorporated by the garnet structure (Geiger, 2004; Rager et al., 2003). However, despite the extremely reducing conditions of synthesis, Ti^{4+} constitutes the majority of the titanium content in this synthetic pyrope: Ti^{3+} could not be detected by optical absorption spectroscopy (Geiger et al., 2000; Geiger, 2004). Reduced titanium was only found by means of the hypersensitive technique of electron paramagnetic resonance spectroscopy, and the concentration of Ti^{3+} in this specimen is considered to be very low (Geiger, 2004; Rager et al., 2003). By inference, Ti^{3+} is therefore quite unlikely to occur in natural garnets, which form at significantly higher oxygen fugacities than those in equilibrium with Ti metal or with Ti_2O_3.

X-ray photoelectron spectra of natural Ti-bearing garnet have been interpreted to demonstrate the presence of substantial Ti^{3+} (Malitesta et al., 1995; Schingaro et al., 2004). However, the poor signal-to-noise ratios of these spectra do not support the extensive curve fitting of multiple Ti species presented by these authors (cf. Atuchin et al., 2006; Carley et al., 1987). In contrast, the results of synchrotron-based X-ray absorption spectroscopy are consistent with Ti^{4+} as the valence state of titanium in garnet (de Groot et al., 1992; Farges et al., 1997; Locock et al., 1995; Waychunas, 1986, 1987).

As inspection of oxygen fugacity buffers, and the results both of synthesis experiments and of investigations using X-ray absorption spectroscopy do not support the presence of Ti^{3+} in garnet, it will not be considered further here. Instead, Ti^{4+} is deemed the sole valence state of titanium in garnet, in agreement with the preponderance of experimental evidence.

2.4. Structure and site occupancies

It is possible to view the chemical substitutions that occur in garnet from the perspective of chemical exchange vectors (Burt, 1991). Such an approach does not explicitly take into account the crystal chemistry of garnet, and may mislead the unwary as to the nature of the complex substitutions (both homovalent and coupled-heterovalent) that occur. In this work, the chemical substitutions in garnet are instead considered in the context of its crystal structure.

In the structure of anhydrous cubic garnets, general formula $\{X_3\}[Y_2](Z_3)\phi_{12}$, space group *Ia*3*d* (#230), there are only four symmetrically unique atomic sites (Geller, 1967). Three of these are on special positions fixed by symmetry, and are occupied by cations: the *X* site is on Wyckoff position 24*c*, the *Y* site corresponds to Wyckoff position 16*h* and the *Z* site occupies Wyckoff position 24*d*. The fourth site is on a general position, 96*h*, and is usually occupied by oxygen, and more rarely by fluorine (Chakhmouradian et al., 2008 and references therein; Smyth et al., 1990). The positional coordinates of the anion site can be related to the mean ionic radii of the cations in the structure (Hawthorne, 1981; Novak and Gibbs, 1971). As described by Deer et al. (1997), "the structure consists of alternating ZO_4 tetrahedra and YO_6 octahedra which share corners to form a three-dimensional framework…. Within this there are cavities that can be described as distorted cubes, or alternatively as triangular dodecahedra, of eight oxygens [anions] which contain the *X* ions."

In hydrous garnets, the major mechanism of hydrogen incorporation is by coupled substitution of H with tetrahedral vacancies in place of Si (Ferro et al., 2003; Lager et al., 1989). In such garnets (in the case of cubic symmetry), the tetrahedral site is not fully occupied, and H partially occupies a separate site of general symmetry, Wyckoff position 96*h*, giving rise to the hydrogarnet substitution mechanism: $(O_4H_4)^{4-} = (SiO_4)^{4-}$ (Ferro et al., 2003; Lager et al., 1989). From a purely chemical point of view, this can be considered a direct substitution in the form: $H_4^{4+} = Si^{4+}$, and for convenience this simplification has been adopted in the spreadsheet. Some hydrous garnets show optical evidence of lower symmetry, which may result from cation ordering in the structure (Kingma and Downs, 1989; Pertlik, 2003). Lower symmetry may help explain observations of complexity in the OH-stretching region of the infrared absorption spectra of some hydrous garnets (Amthauer and Rossman, 1998; Pertlik, 2003). Such spectral complexity has been construed alternatively as indicating additional types of H incorporation (Libowitzky and Beran, 2004), but the hydrogarnet substitution is nevertheless widely accepted as the dominant mechanism. The occurrence of significant vacancies on the {*X*} and [*Y*] sites is not well supported by the literature and is not considered here. The hydrous garnet-related minerals henritermierite, $\{Ca_3\}[Mn_2^{3+}](SiO_4)_2(OH)_4$ (Armbruster et al., 2001) and holtstamite, $\{Ca_3\}[(Al,Mn^{3+})_2](SiO_4)_2(OH)_4$ (Hålenius et al., 2005) have tetragonal symmetry, but are closely related to the cubic garnet structure, and may be considered, for the purposes of this work, to be examples (in a chemical sense) of the hydrogarnet substitution.

In natural silicate garnets, fluorine can substitute for oxygen with charge balance maintained by vacancies in the tetrahedral site (Chakhmouradian et al., 2008 and references therein; Smyth et al., 1990). This is in contrast to the tetrahedral Li content observed for cryolithionite, $\{Na_3\}[Al_2](Li_3)F_{12}$ (Menzer, 1927).

The site preferences of the cations (H, Na, Mg, Al, Si, Ca, Sc, Ti, V, Cr, Mn^{2+}, Mn^{3+}, Fe^{2+}, Fe^{3+}, Y, Zr and Sn) for the dodecahedral {*X*}, octahedral [*Y*] and tetrahedral (*Z*) sites have been reported in the literature from the results of many crystal structure refinements and spectroscopic investigations of silicate garnets, and isostructural species such as berzeliite, $\{Ca_2Na\}[Mg_2](As_3)O_{12}$ (cf. Amthauer et al., 1979; Chakhmouradian et al., 2008; Deer et al., 1997; Galuskina et al., 2005; Geller, 1967; Hawthorne, 1981; Novak and Gibbs, 1971; Smyth et al., 1990). The site occupancies used in the

spreadsheet follow (listed for each cation site in order of increasing atomic number):

$\{X\}$ = Na, Mg, Ca, Mn^{2+}, Fe^{2+}, Y;

$[Y]$ = Mg, Al, Si, Sc, Ti, V, Cr, Mn^{3+}, Fe^{2+}, Fe^{3+}, Zr, Sn;

(Z) = Al, Si, Fe^{3+}, the hydrogarnet substitution: H_4, and vacancies associated with F content;

φ = O, F.

As the purpose of this spreadsheet program is to recast garnet analyses into their most abundant and common end-member components, this scheme of site occupancies does not take into account controversial or rare site assignments such as divalent iron on the tetrahedral site, (Fe^{2+}), or divalent manganese on the octahedral site, [Mn^{2+}]. In particular, Ti is assigned solely to the octahedral [*Y*] site, and is considered to occur only as Ti^{4+}, as discussed above. In addition, although Sc has been shown in synthetic systems to have mechanisms of substitution that depend on the bulk composition of the garnet (Oberti et al., 2006; Quartieri et al., 2006), for simplicity, Sc has been assigned solely to the octahedral [*Y*] site, in agreement with results for natural and synthetic Ca-rich scandian garnets (Galuskina et al., 2005; Quartieri et al., 2006).

Several cations can occupy more than one crystallographic site in the garnet structure (e.g., Mg, Al, Si, Sc, Fe^{2+}, Fe^{3+}). In principle, their distribution between sites should be determined by crystal structure refinement and/or spectroscopic methods in combination with their abundances. However, it must be emphasized that as the current work depends on calculation solely from chemical analyses, some reasonable restrictions must instead be applied, the details of which are discussed in Section 4. Similarly, although both Mn and Fe can adopt more than one valence state, the relative concentrations of which can be measured by spectroscopic or chemical methods, most analyses of garnet do not distinguish between the valence states and instead provide only the total concentrations of each element. For such cases, the proportions of Mn^{2+}, Mn^{3+}, Fe^{2+} and Fe^{3+} are calculated by stoichiometric constraints (Droop, 1987) as reported in Section 4.

3. Garnet end-members

The 15 mineral species of the garnet group form the basis from which to determine the end-member components necessary to describe the chemical complexity of natural garnets. Mineral species are generally defined in accordance with the dominance principle of the (recently renamed) Commission on New Minerals, Nomenclature and Classification (CNMNC) of the International Mineralogical Association: a mineral species is defined by the predominant atoms that occupy its various structural sites (Nickel and Grice, 1998). The CNMNC does not require the author(s) of a new mineral species to report an end-member formula. As detailed by Hawthorne (2002), the requirements for an end-member formula are more rigorous: (1) the chemical formula must be fixed, (2) the formula must be compatible with the crystal structure and (3) the chemical composition at each structural site must be fixed; an end-member formula may have two types of cation or anion (in a fixed ratio) at one structural site if required for electroneutrality; two cations or anions at more than one site are not allowed.

Many of the formulas of the mineral species of the garnet group are expressed commonly as end-members: almandine, $\{Fe_3^{2+}\}[Al_2](Si_3)O_{12}$; andradite, $\{Ca_3\}[Fe_2^{3+}](Si_3)O_{12}$; calderite, $\{Mn_3^{2+}\}[Fe_2^{3+}](Si_3)O_{12}$; goldmanite, $\{Ca_3\}[V_2](Si_3)O_{12}$; grossular, $\{Ca_3\}[Al_2](Si_3)O_{12}$; knorringite, $\{Mg_3\}[Cr_2](Si_3)O_{12}$; morimotoite, $\{Ca_3\}[TiFe^{2+}](Si_3)O_{12}$; pyrope, $\{Mg_3\}[Al_2](Si_3)O_{12}$; spessartine, $\{Mn_3\}[Al_2](Si_3)O_{12}$; and uvarovite, $\{Ca_3\}[Cr_2](Si_3)O_{12}$ (Mandarino and Back, 2004). For the remaining mineral species, idealized end-members have been assumed for the purposes of this work in accord with the requirements set forth by Hawthorne (2002). Thus, the katoite end-member is defined here as $\{Ca_3\}[Al_2](OH)_{12}$; kimzeyite, $\{Ca_3\}[Zr_2](SiAl_2)O_{12}$; majorite, $\{Mg_3\}[MgSi](Si_3)O_{12}$; and schorlomite, $\{Ca_3\}[Ti_2](SiFe_2^{3+})O_{12}$. It should be noted that Chakhmouradian and McCammon (2005) have discussed in detail the topic of the proper formula and interspecies boundaries for schorlomite, and concluded that this species cannot be entirely represented by a single end-member formula and is best expressed in general form as: $\{Ca_3\}[Ti_2^{4+}](Si_{3-x})(Fe^{3+},Al,Fe^{2+})_xO_{12}$. The current work is mainly in agreement with such conclusions with regard to the mineral species; from consideration of the chemical data in the literature, the compositions of Ti-rich silicate garnets may require up to six Ti-bearing end-member components for their description. The dominant component in the generalized species formula of Chakhmouradian and McCammon (2005) is $\{Ca_3\}[Ti_2](SiFe_2^{3+})O_{12}$, and for convenience, this is referred to herein as the schorlomite end-member. Morimotoite, $\{Ca_3\}[TiFe^{2+}](Si_3)O_{12}$, is the only other Ti-bearing end-member that corresponds to an actual mineral species. The four hypothetical end-members that are also needed (with their names shown in italics to reinforce that they are *not* mineral species names) are: *schorlomite-Al*, $\{Ca_3\}[Ti_2](SiAl_2)O_{12}$; *morimotoite-Mg*, $\{Ca_3\}[TiMg](Si_3)O_{12}$ (the Mg-melanite of Platt and Mitchell, 1979); *morimotoite-Fe*, $\{Fe_3^{2+}\}[TiFe^{2+}](Si_3)O_{12}$; and *NaTi garnet*, $\{Na_2Ca\}[Ti_2](Si_3)O_{12}$. The Na content of some silicate garnets has been suggested to be related to heterovalent substitutions involving Y or P (e.g., Enami et al., 1995), but is expressed here by the end-member *NaTi garnet*, $\{Na_2Ca\}[Ti_2](Si_3)O_{12}$, as the Ti-rich garnets are frequently both Na-bearing and Ca-rich (Deer et al., 1997). The assignment of this end-member is also supported by analyses of pyrope-rich garnets from Bohemia, in which Na content is positively correlated with increasing Ti content (Seifert and Vrána, 2005).

From the perspective of end-members, the species hibschite—$\{Ca_3\}[Al_2](SiO_4)_{3-x}(OH)_{4x}$, $0.2 < x < 1.5$—can be expressed as a mixture of grossular and katoite components. Similarly, from a purely chemical point of view, although henritermierite, $\{Ca_3\}[Mn_2^{3+}](SiO_4)_2(OH)_4$, can be adopted as an end-member component, the related

tetragonal species holtstamite, $\{Ca_3\}[(Al,Mn^{3+})_2](SiO_4)_2(OH)_4$, is not an end-member as it can be represented compositionally as a mixture of grossular, katoite and henritermierite components.

Aside from the mineral species, and the various end-members required by the presence of Ti, several hypothetical end-members (some of which have long-established informal names) are also required to accommodate the range of major-element compositions of natural garnets including: *blythite*, $\{Mn_3^{2+}\}[Mn_2^{3+}](Si_3)O_{12}$; *khoharite*, $\{Mg_3\}[Fe_2^{3+}](Si_3)O_{12}$; *kimzeyite-Fe*, $\{Ca_3\}[Zr_2](SiFe_2^{3+})O_{12}$ (the ferric-kimzeyite of Rickwood, 1968); *skiagite*, $\{Fe_3^{2+}\}[Fe_2^{3+}](Si_3)O_{12}$; *yamatoite*, $\{Mn_3\}[V_2](Si_3)O_{12}$; and *yttrogarnet*, $\{Y_3\}[Al_2](Al_3)O_{12}$ (known commonly in the solid-state science literature as *YAG*). The Sc end-member is taken to be $\{Ca_3\}[Sc_2](Si_3)O_{12}$ (Galuskina et al., 2005; Quartieri et al., 2006), whereas the mechanism of Sn incorporation is similar to that of Ti in morimotoite: $\{Ca_3\}[SnFe^{2+}](Si_3)O_{12}$ (Amthauer et al., 1979). Two fluorine-bearing end-members (with completely vacant tetrahedral sites) are required, based on structure refinements of natural specimens (Chakhmouradian et al., 2008; Smyth et al., 1990): $\{Ca_3\}[Al_2]( )_3F_{12}$ and $\{Mn_3\}[Al_2]( )_3F_{12}$, respectively, where ( ) = vacancy.

The complete list of end-member components (Table 1) differs from those established by Rickwood (1968) because of the greater range of elements considered and the different treatment of H, Mn^{3+}, Ti and octahedral Si.

Table 1
Cation site occupancies for garnet end-members

End-members[a]	Dodecahedral	Octahedral	Tetrahedral	Anion
Henritermierite	Ca_3	Mn_2^{3+}	$Si_2(H_4)$	O_{12}
Blythite	Mn_3^{2+}	Mn_2^{3+}	Si_3	O_{12}
Katoite	Ca_3	Al_2	$(H_4)_3$	O_{12}
FCa garnet	Ca_3	Al_2	$( )_3$	F_{12}
FMn garnet	Mn_3	Al_2	$( )_3$	F_{12}
Yttrogarnet (YAG)	Y_3	Al_2	Al_3	O_{12}
Kimzeyite	Ca_3	Zr_2	$SiAl_2$	O_{12}
Kimzeyite-Fe	Ca_3	Zr_2	$SiFe_2^{3+}$	O_{12}
Tin garnet	Ca_3	$SnFe^{2+}$	Si_3	O_{12}
Schorlomite	Ca_3	Ti_2	$SiFe_2^{3+}$	O_{12}
Schorlomite-Al	Ca_3	Ti_2	$SiAl_2$	O_{12}
Morimotoite	Ca_3	$TiFe^{2+}$	Si_3	O_{12}
NaTi garnet	Na_2Ca	Ti_2	Si_3	O_{12}
Morimotoite-Mg	Ca_3	TiMg	Si_3	O_{12}
Morimotoite-Fe	Fe_3^{2+}	$TiFe^{2+}$	Si_3	O_{12}
Majorite	Mg_3	MgSi	Si_3	O_{12}
Sc garnet	Ca_3	Sc_2	Si_3	O_{12}
Goldmanite	Ca_3	V_2	Si_3	O_{12}
Yamatoite	Mn_3^{2+}	V_2	Si_3	O_{12}
Uvarovite	Ca_3	Cr_2	Si_3	O_{12}
Knorringite	Mg_3	Cr_2	Si_3	O_{12}
Spessartine	Mn_3^{2+}	Al_2	Si_3	O_{12}
Pyrope	Mg_3	Al_2	Si_3	O_{12}
Almandine	Fe_3^{2+}	Al_2	Si_3	O_{12}
Grossular	Ca_3	Al_2	Si_3	O_{12}
Andradite	Ca_3	Fe_2^{3+}	Si_3	O_{12}
Calderite	Mn_3^{2+}	Fe_2^{3+}	Si_3	O_{12}
Skiagite	Fe_3^{2+}	Fe_2^{3+}	Si_3	O_{12}
Khoharite	Mg_3	Fe_2^{3+}	Si_3	O_{12}

[a] Mineral names listed in regular font, hypothetical end-members in italics.

4. Spreadsheet description

The Excel spreadsheet consists of six worksheets. The main three worksheets include the **Instructions** worksheet, the **Data** worksheet that contains both the input chemical data and the output molar proportions of end-members, and the **Calculation** worksheet in which the details of the cation assignments and calculation of the end-members have been programmed. The remaining three worksheets contain compositional data from both Deer et al. (1997) and from the literature. In worksheet **DHZ**, results are calculated for 250 analyses listed by Deer et al. (1997), with the proportions of Fe^{2+} and Fe^{3+} maintained as originally reported. In worksheet **DHZferrous**, the results are calculated for the same set of 250 analyses but with the Fe contents taken to be initially Fe^{2+} and the final proportions of Fe^{2+} and Fe^{3+} calculated by stoichiometry. The **Literature** worksheet lists compositional data and results for an additional 220 analyses taken from 27 literature references: (Amthauer et al., 1979; Armbruster et al., 1998; Berger et al., 2005; Boctor et al., 1982; Bühn et al., 1995; Cenki-Tok and Chopin, 2006; Chakhmouradian and McCammon, 2005; Chakhmouradian et al., 2008; Dwarzski et al., 2006; Enami et al., 1995; Ferro et al., 2003; Flohr and Ross, 1989; Galuskina et al., 2005; Geiger and Armbruster, 1997; Hålenius, 2004; Labotka, 1995; Locock et al., 1995; Luth et al., 1990; Platt and Mitchell, 1979; Quartieri et al., 2002; Seifert and Vrána, 2005; Smith and Mason, 1970; Smyth et al., 1990; Stachel, 2001; Stachel et al., 2006; Tappert et al., 2005; Uher et al., 1994).

4.1. Data input

Compositional data are entered as oxides in weight percent (preferably to two decimal places) in the columns of the **Data** worksheet, as illustrated in Table 2 with select analyses from Friberg (1989), Knowles (1987), Muhling and Griffin (1991) and Rickwood (1968). Up to 100 analyses can be entered in the **Data** worksheet. The user should assign to each chemical analysis a unique identifying label in the cell above the SiO_2 content to enable quick location of that analysis in the **Calculation** worksheet. In the examples shown in Table 2, the labels used correspond to the publication dates. Unless the proportions of FeO and Fe_2O_3 have been determined, the iron content should be entered as FeO_{tot}. In the case of manganese, the entire content must be entered as MnO; the (Mn_2O_3) field shown is only a placeholder for calculations taking place elsewhere in the spreadsheet. The correction for O = F and the total are calculated in the worksheet and should not be entered by the user.

4.2. Atomic proportions and charge balance

In the **Calculation** worksheet, the analyses input in the columns of the **Data** worksheet are reproduced automatically. For each individual analysis, the atomic proportions of the elements are calculated in the following manner: molar proportions of the cations, oxygen and

Table 2
Examples of input data for garnet analyses

Analysis (wt%)	Rickwood (1968)	Knowles (1987)	Friberg (1989)	Muhling and Griffin (1991)
SiO_2	41.97	37.39	41.50	41.40
TiO_2	0.24	0.16	0.08	0.42
ZrO_2				
SnO_2				
Y_2O_3				
Al_2O_3	21.73	20.72	22.35	20.00
Sc_2O_3				
Cr_2O_3	0.72			3.85
V_2O_3				
FeO/ FeO_{tot}[a]	6.17	36.37	14.56	7.50
Fe_2O_3/calc	2.36	0.83	0.95	
MnO (Mn_2O_3)[b]	0.97	0.86	0.29	0.34
MgO	20.45	3.85	14.82	21.50
CaO	5.52	0.41	5.36	4.50
Na_2O				0.12
H_2O+	0.02		0.36	
F				
O=F (calc)				
Total (calc)	100.15	100.59	100.27	99.63

[a] Enter all Fe as FeO_{tot} unless both FeO and Fe_2O_3 are known.
[b] Enter all Mn as MnO only; (Mn_2O_3) field is a placeholder.

fluorine are calculated from the weight-percent values; the molar proportions are converted to atoms per formula unit (apfu) on the basis that the sum of the cations (including vacancies in the tetrahedral site associated with the presence of F) is set to exactly 8 apfu. In this calculation, hydrogen is treated as a cation (H_4^{4+}) for convenience. It should be noted that Excel carries numerical values to more than 10 decimal places in its calculations, and no truncation or rounding takes place in the spreadsheet until the report of the end-member proportions.

For chemical analyses in which both FeO and Fe_2O_3 are given, exact electroneutrality will be achieved only infrequently in the calculation of the atomic proportions. Therefore, the sum of the oxygen will generally deviate slightly from 12 apfu (either higher or lower than 12). This deviation is reported on the **Calculation** worksheet as either an excess or a deficit of O pfu, along with a caution that the analysis does not charge balance.

Following Droop (1987), for the analyses in which the iron content has been input solely as FeO, stoichiometric constraints are used to calculate the proportions of Fe^{2+} and Fe^{3+} (and Mn^{3+}, if necessary). If all of the iron content is presented initially as Fe^{2+} and an oxygen surplus still results, all of the iron is kept as Fe^{2+}, no Mn^{3+} is calculated, and the caution that the analysis does not charge balance is reported. If the iron content has been input solely as FeO, and an oxygen deficit is calculated initially, then some or all of the iron (as necessary) is recalculated as Fe^{3+} in an attempt to achieve electroneutrality. If charge balance still has not been reached with the entire iron content recalculated as Fe^{3+}, some or all of the manganese is recalculated as Mn^{3+}.

4.3. Assignment of cations to crystallographic sites

In order to assign elements without ambiguity to the three cation sites in the garnet structure, certain simplifying assumptions must be made and restrictions imposed. For example, Fe^{2+} generally occurs in the dodecahedral {*X*} site (e.g., almandine), and also in the octahedral [*Y*] site (e.g., morimotoite), and although it has been reported to occur in the tetrahedral (*Z*) site in certain Ti-rich garnets (Locock et al., 1995), this interpretation has been questioned (Chakhmouradian and McCammon, 2005). For this reason, and due to the difficulty in determining the distribution of a given element among three sites (in the absence of spectroscopic or site-refinement data), each element of a given valence state is restricted in this scheme to either one or two sites. The cations are allocated to the tetrahedral (*Z*) site as follows:

- the entire hydrogen content is assigned as H_4 and this moiety treated as a single cation;
- if F is present, tetrahedral vacancies, $(\ )_F$, are assigned in the proportion 0.25 F apfu;
- if the entire content of Si > 3 apfu, then 3 Si are assigned here, with the remaining Si placed on the octahedral [*Y*] site. (Only with inferior analyses of hydrous garnets will the case occur where Si > 3 apfu in the presence of hydrogen);
- if $Si+(\ )_F+H_4 < 3$ apfu, then Al is used to fill the remainder of the (*Z*) site, if possible;
- if necessary, Fe^{3+} is finally used to fill the remainder of the tetrahedral site.

The octahedral [*Y*] site is filled in the following fashion:

- any Si in excess of 3 apfu is assigned to this site;
- all of the Ti, Zr, Sn, Sc, Cr, V and Mn^{3+} are allocated here;
- the Al and Fe^{3+} remaining after the completion of the (*Z*) site are assigned;
- Mg may be assigned here if Si is present on this site, or if the sum of the entire contents of $Mg+Ca+Mn^{2+}+Na$ exceed 3 apfu;
- if necessary, Fe^{2+} is used to fill the remainder of the octahedral site.

The dodecahedral {*X*} site has the following cation assignments:

- all of the Na, Ca, Mn^{2+} and Y are allocated here;
- all of the remaining Mg and Fe^{2+} are assigned to this site.

Table 3 shows the example of an analysis quoted by Friberg (1989) with its cation assignments. The sums for the dodecahedral and octahedral site are not quite ideal (as a result of the inflexible allocation of the various cations), which is flagged in the **Calculation** worksheet by the caution: "cation proportions not ideal". As this analysis does not achieve exact electroneutrality, the nature and magnitude of the deviation are marked

Table 3
Assignment of cations to crystallographic sites (analysis of Friberg, 1989)

Chemical analysis	1989 wt% oxide	Cations	Cation assignments (apfu)		
			Dodecahedral	Octahedral	Tetrahedral
SiO_2	41.50	Si		0.0327	3.0000
TiO_2	0.08	Ti		0.0044	
ZrO_2	0.00	Zr		0.0000	
SnO_2	0.00	Sn		0.0000	
Y_2O_3	0.00	Y	0.0000		
Al_2O_3	22.35	Al		1.9249	0.0000
Sc_2O_3	0.00	Sc		0.0000	
Cr_2O_3	0.00	Cr		0.0000	
V_2O_3	0.00	V		0.0000	
FeO/FeO_{tot}	14.56	Fe^{2+}	0.8898	0.0000	
Fe_2O_3/calc	0.95	Fe^{3+}		0.0522	0.0000
MnO	0.29	Mn^{2+}	0.0179		
(Mn_2O_3)	0.00	Mn^{3+}		0.0000	
MgO	14.82	Mg	1.6145	0.0000	
CaO	5.36	Ca	0.4197		
Na_2O	0.00	Na	0.0000		
H_2O+	0.36	H_4			0.0439
F	0.00	*vac* ( )			*0.0000*
O=F (calc)		Subtotal	2.9419	2.0142	3.0439
Total (calc)	100.27		Cation proportions not ideal		
				Fe^{3+}/Fe_{tot}	5.55%
				Mn^{3+}/Mn_{tot}	0.00%
		0.070	O excess pfu, does not charge balance		
		O anions	12.0695		
		F anions	0.0000		

by the caution "0.070 O excess pfu, does not charge balance".

4.4. Sequential calculation of end-member proportions

In the **Calculation** worksheet, the end-member proportions are generated by successive calculation in the order shown in Table 1. This sequence was determined from several considerations: the imperative to minimize the number and proportions of hypothetical end-members, the desire to represent minor chemical constituents (e.g., Na) by plausible end-members, and the requirement for the results to be in substantial agreement with those generated by the procedure of Rickwood (1968) despite the wider range and somewhat different sequence of end-members used here. In schemes that involve serial calculation, the sequence will always influence the results, as discussed in some detail by Rickwood (1968), who emphasized the need for a standard method of calculation. The details of the calculation sequence used in the spreadsheet are described below.

In the garnet structure, the tetrahedral site has the highest bond-valence, and so substitutions on this site (H, Al, Fe and vacancies in place of Si) are assigned precedence. As hydrogen is presumed not to be involved with substitutions on any other sites, the hydrogen-bearing end-members are assigned first. As henritermierite also requires the uncommon constituent [Mn^{3+}], it is calculated before katoite and is followed by *blythite*, as it is the only other component that requires [Mn^{3+}]. The other hydrogen-bearing end-member, katoite, is then calculated, followed by the fluorine-bearing end-members (in the order Ca, Mn), and then by *yttrogarnet*.

The octahedral cation site has the next-highest bond-valence in the garnet structure, and substitutions involving this site guide the ordering of the remaining end-members in the sequence. These are generally organized in order of decreasing valence state and decreasing ionic radius of the octahedral cations: Zr^{4+}, Sn^{4+}, Ti^{4+}, Sc^{3+}, V^{3+}, Cr^{3+}, Al^{3+}, but with the Fe^{3+} end-members located at the end of the sequence. This placement results from an attempt to reduce propagated analytical uncertainty. The entire analytical uncertainty associated with a chemical analysis is propagated (and magnified) in the calculation from stoichiometric constraints of the proportion of Fe^{3+}, and it can therefore be expected that the Fe^{3+} end-members will inherently have higher relative uncertainty. Their placement at the end of the calculation sequence therefore minimizes the effects of error propagation on the calculation of the other end-members.

For a given octahedral cation, the end-members are organized by the nature of their substitutions and their perceived abundance in natural systems. Thus, for Zr, kimzeyite is calculated before *kimzeyite-Fe*. In the case of Ti, schorlomite and *schorlomite-Al*, both of which have substitutions on the tetrahedral site, are calculated before morimotoite, *NaTi garnet*, *morimotoite-Mg* and *morimotoite-Fe*. The calculation of majorite immediately after the Ti end-members is an exception to the arrangement of decreasing valence state and ionic radius for the octahedral cations. It follows the Ti-bearing morimotoite-type end-members (Table 1), and has a similar coupled substitution on the octahedral site: [$Y^{4+}Y^{2+}$], where

Y^{4+} = Ti for the morimotoite-type end-members with Y^{2+} = Fe or Mg, and Y^{4+} = Si for majorite with Y^{2+} = Mg. In the cases of the V- and Cr-bearing end-members, the order again reflects their perceived abundance in natural systems: goldmanite comes before *yamatoite*, and uvarovite comes before knorringite. For the Al-bearing end-members, pyrope and almandine are calculated before grossular and andradite. As more than half of the end-members in Table 1 are Ca-bearing, as a result of error propagation by the end of the calculation sequence the Ca-bearing end-members are expected to have higher relative uncertainty than the other end-members. Pyrope and almandine are therefore determined prior to grossular and andradite to avoid unnecessarily increasing the uncertainty of the former two end-members. Finally, the Fe^{3+}-bearing end-members are also arranged by their perceived abundance in natural systems: andradite, calderite, *skiagite* and *khoharite*.

4.5. Data output

The proportions of the garnet end-members determined in the **Calculation** worksheet are expressed as percentages (rounded to two decimal places), and are reproduced automatically in the **Data** worksheet, below the chemical analysis with which they correspond. The results calculated for the select analyses listed in Table 2 can be found in Table 4, along with the end-member proportions presented by the original authors and by Deer et al. (1997) for the same chemical data. The calculation scheme used in the current spreadsheet yields results similar to those of Deer et al. (1997), Friberg (1989), Knowles (1987), Rickwood (1968) and Yang (1991), despite the wider range of composition considered here, and the somewhat different set and order of end-members used in the spreadsheet. The most significant differences involve the presence of Ti-bearing end-members, and the explicit calculation in the spreadsheet of a remainder—the proportion of cations that could not be allocated to any electroneutral end-member.

In contrast, there are considerable differences between the results from the current procedure, and those generated by the method of Muhling and Griffin (1991). These discrepancies are attributable mainly to the different treatment of Cr in the latter method. Their scheme under-estimates the amount of uvarovite and consequently inflates the quantity of knorringite; this also results in an under-estimate of pyrope, and an over-estimate of almandine and andradite. It is considered preferable in the current work to follow Rickwood (1968), and maximize the proportion of uvarovite relative to knorringite, in agreement with their perceived abundances in natural systems.

4.6. Remainder and quality index

Almost all garnet analyses are imperfect: the analytical sum may be outside normal ranges, the proportion of cations allocated to a given site may be too high or too low, the amount of Si may be greater than 3 apfu in a

Table 4
Comparison of end-member proportions between current work, original references and Deer et al. (1997)

Source	Rickwood (1968)			Yang (1991)	Knowles (1987)			Friberg (1989)			Muhling and Griffin (1991)		
	Current	Original	DHZ-3 Prp		Current	Original	DHZ-3 Alm	Current	Original	DHZ-18 Prp	Current	Original	DHZ-2 Cr-Prp
Katoite	0.08	0.00	0.0	0.0				1.46	0.0	1.6			
Schorlomite-Al	0.64	0.00	0.0	0.0	0.26	0.00	0.0				1.13	1.14	0.0
Uvarovite	2.02	2.04	2.0	2.0							10.35	4.95	11.4
Knorringite											0.52	6.00	0.0
Spessartine	1.95	1.96	2.0	2.0	1.94	1.97	1.9	0.60	0.6	0.6	0.69	0.25	0.7
Pyrope	72.25	72.67	72.7	72.3	15.32	15.48	15.4	53.82	54.9	54.9	75.79	70.81	80.1
Almandine	11.79	11.27	11.3	11.7	80.27	81.37	80.8	29.66	30.2	30.3	5.57	11.39	7.2
Grossular	4.30	5.71	5.7	5.7				10.71	11.4	9.9	0.00	0.00	0.6
Andradite	6.31	6.35	6.4	6.3	0.91	1.19	1.2	1.82	2.9	2.7	0.00	5.48	0.0
Skiagite					0.94	0.00	0.7				4.17	0.00	0.0
Remainder	0.66	0.00	0.0	0.0	0.35	0.00	0.0	1.94	0.0	0.0	1.78	0.00	0.0
Total	100.00	100.00	100.1	100.0	99.99	100.01	100.0	100.01	100.0	100.0	100.00	100.02	100.0

Note: End-members with null values for all entries have been omitted.

Table 5
Remainder after calculation of end-members (analysis of Friberg, 1989)

Remainder (*apfu*)			
Cations	Dodecahedral	Octahedral	Tetrahedral
Si		0.0327	0.1019
Ti		0.0044	
Zr			
Sn			
Y			
Al			
Sc			
Cr			
V			
Fe^{2+}			
Fe^{3+}		0.0159	
Mn^{2+}			
Mn^{3+}			
Mg			
Ca			
Na			
H_4			
Subtotal		0.0529	0.1019

garnet that should not have a majorite component, or the analysis may not charge balance. It is for such reasons that, after the proportions of the end-members have been calculated, there are often cations left over that could not be allocated: the remainder. In the case of the analysis of Friberg (1989) presented in Tables 2–4, the remainder sums to 1.94%. The details of the remainder for a given analysis are given in the **Calculation** worksheet. Table 5 displays the remainder for the analysis of Friberg (1989), in which it can be seen that the 1.94% remainder corresponds to: unallocated Si (on both the tetrahedral and octahedral sites); Ti that could not be allocated to an end-member (schorlomite-type end-members require a coupled substitution with the tetrahedral site that is prevented by the surplus Si, morimotoite-type end-members require a coupled substitution on the octahedral site that is prevented by the surplus octahedral cations); and surplus Fe^{3+}. Inspection of the remainder of a given analysis may assist the user in detecting an undescribed component, or may indicate possible analytical difficulties. However, the magnitude and nature of the remainder alone is not a sufficient measure of the quality of a garnet analysis.

In order to have some objective measure of quality, a simple scoring algorithm, referred to as the Quality Index, is calculated in the **Data** worksheet for each analysis. The Quality Index takes into account the original analytical total, the deviation from ideality of the cation proportions, the presence of superfluous octahedral Si, the extent of charge balance and the magnitude of the remainder. The vocabulary of the Quality Index is based on the compatibility concept used in Gladstone-Dale calculations (Mandarino, 1981), and is calculated as follows:

- if the analytical total is outside the range of 97–101%, add 1 point
- if the proportions for one or more cation sites are not ideal, add 1 point
- if octahedral Si is present for an analysis with dodecahedral Mg <0.75 apfu, add 1 point (majorite should only occur in Mg-rich analyses)
- if the analysis does not charge balance, add 1 point
- if the magnitude of the remainder is: $>8\%$, add 5 points; $>4\%$, add 3 points; $>2\%$, add 2 points; $>1\%$, add 1 point
- for a given point total, the Quality Index designation is: 0–1, superior; >1, excellent; >2, good; >3, fair; >4, poor.

If an analysis merits a Quality Index of "poor" (or even "fair"), the remainder should likely be examined in detail, and consideration should be given to possible analytical difficulties encountered during data acquisition.

5. Testing of the spreadsheet

In order to test the capability and utility of the spreadsheet, 250 garnet analyses tabulated in Deer et al. (1997) were entered, disregarding any atypical contents such as P, K, Ni or Zn, etc. End-member proportions were calculated both for the analyses with the proportions of Fe^{2+} and Fe^{3+} maintained as originally reported (worksheet **DHZ**), and for the same analyses but with the Fe contents taken to be initially Fe^{2+} and the final proportions of Fe^{2+} and Fe^{3+} calculated by stoichiometry (worksheet **DHZferrous**). In general, the end-member proportions are similar to those presented by Deer et al. (1997). Interestingly, the values of the Quality Index in the **DHZferrous** worksheet are often slightly more favorable than in the **DHZ** worksheet, likely because the calculation of Fe^{2+} and Fe^{3+} from stoichiometry allows the results to more easily charge balance and to more closely approach ideal cation proportions.

A further 220 analyses, mostly electron-microprobe data, from 27 literature references (cited above in Section 4) are tabulated in the **Literature** worksheet, covering a wide range of compositions. Inspection of these data reveals that the end-member *morimotoite-Mg*, $\{Ca_3\}[TiMg](Si_3)O_{12}$, is apparently the dominant component in several garnet analyses (using the sequence of calculation shown in Table 1), and that this hypothetical component may therefore require species status. The end-member *morimotoite-Mg* is most frequently found in Ti-bearing garnets (e.g., Armbruster et al., 1998; Chakhmouradian and McCammon, 2005; Flohr and Ross, 1989; Labotka, 1995; Locock et al., 1995; Quartieri et al., 2002), and is the most abundant component in ten of the 16 analyses (with a maximum of 29.4%) of Platt and Mitchell (1979), and is a similarly major component in their remaining six analyses. Further investigation, ideally involving spectroscopic and structural data, is needed to determine whether *morimotoite-Mg* should be awarded the status of a mineral species.

5.1. Propagation of analytical uncertainty

Rigorous evaluation of the propagation of analytical uncertainty from the initial chemical data through to the

calculation of the end-member proportions is beyond the scope of this work; only a brief discussion of error propagation follows. Giaramita and Day (1990) presented a thorough analysis of error propagation in the calculation of a structural formula, and noted that the "uncertainty in multisite and multivalent cations cannot be estimated directly from the uncertainty in the corresponding oxide concentrations." Rather, partial-, or preferably, complete-error propagation methods are required. Even so, uncertainties in the structural formula (and thereby the end-member proportions) are commonly magnified in a complex fashion. According to Giaramita and Day (1990), such "error magnification depends not only on the composition of the mineral, the normalization scheme used and the structural formula to which the cations are assigned, but also on the relative sizes of uncertainties in the oxides and the contribution of covariance".

As an example of error propagation and magnification, the chemical analysis of a quinary garnet, almandine-grossular-spessartine-pyrope-andradite (#48 from Table 55 of Deer et al., 1997), was assigned a Gaussian distribution of analytical uncertainty (Table 6). The mean was set equal to the original data set, a standard deviation of ~1% relative error was assigned to the major oxides and a standard deviation of ~5% relative error was assigned to the minor oxides (TiO_2, Na_2O) as a proxy for the analytical uncertainty expected in a set of high-quality analyses obtained with the use of an electron microprobe. The end-member proportions were calculated for 20,000 trials (i.e., 20,000 fictive electron-microprobe analyses).

As might be expected, the proportions of the major end-members are normally distributed, with low skewness and kurtosis (Table 6), with the exception of pyrope (Fig. 1), which shows a significant tail to low proportions. This tail results from the calculation of majorite prior to pyrope. Majorite and pyrope are almost perfectly anti-correlated in these trials (correlation coefficient −0.992). The relative uncertainty in majorite is very large (317.9%), as it requires both octahedral Si and octahedral Mg, which only occur occasionally (15.5% of the trials) because of fortuitous statistical fluctuations in the set of 20,000 trials (Fig. 2). The uncertainty in the proportion of majorite affects the amount of Mg remaining available to calculate pyrope, and thus magnifies its uncertainty in turn.

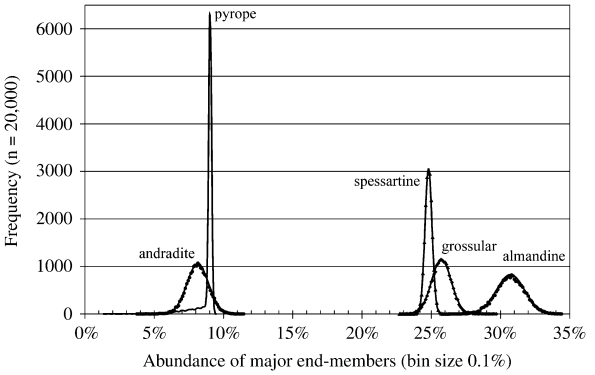

Fig. 1. Propagation of analytical uncertainty for major components: distribution of proportions of andradite, pyrope, spessartine, grossular and almandine in 20,000 trials. Both raw data (symbols) and ideal Gaussian curves are shown for each component, except for pyrope, for which only a raw curve is exhibited.

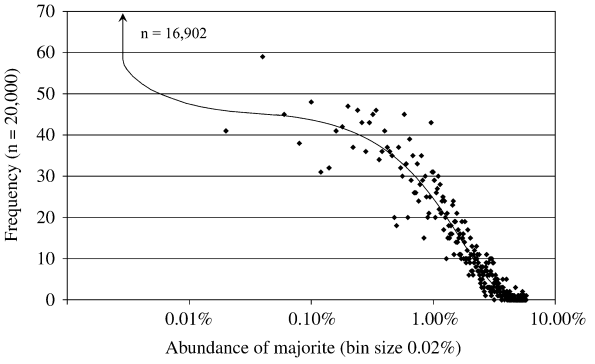

Fig. 2. Propagation of analytical uncertainty for a minor component: distribution of majorite in 20,000 trials. A best-fit line is shown. Note that 84.5% of trials have less than 0.01 mol% majorite.

Table 6
Example of propagation of error into end-member proportions in a quinary garnet: Gaussian distribution of initial error

Input[a]	SiO_2	TiO_2	Al_2O_3	FeO_{tot}	MnO	MgO	CaO	Na_2O	Total
Initial composition (wt%)	37.75	0.14	19.36	17.04	11.06	2.28	12.04	0.15	99.82
Std deviation (wt%)	0.3782	0.0076	0.1945	0.1699	0.1110	0.0231	0.1204	0.0081	0.4853
Relative error (%)	1.0	5.4	1.0	1.0	1.0	1.0	1.0	5.4	0.5
Output	**Schorlomite-Al**	**NaTi garnet**	**Majorite**	**Spessartine**	**Pyrope[b]**	**Almandine**	**Grossular**	**Andradite**	**Remainder**
Exact result (mol%)[c]	0.32	0.10	0	24.76	8.98	30.68	25.72	8.02	1.41
Average (mol%)[d]	0.23	0.19	0.17	24.76	8.75	30.67	25.69	8.09	1.45
Std deviation (mol%)	0.20	0.20	0.55	0.26	0.75	1.02	0.71	0.78	0.69
Relative error (%)	86.8	103.8	317.9	1.0	8.6	3.3	2.8	9.7	47.3
Skewness	−0.16	0.20	4.12	−0.01	−3.98	−0.04	0.04	−0.10	0.51
Kurtosis	−1.86	−1.85	19.63	0.21	18.58	−0.03	0.33	0.40	−0.63

[a] Analysis #48 from Table 55 of Deer et al. (1997), with all iron expressed as FeO_{tot}.
[b] For 17,290 trials with <0.4% majorite: average 8.99, std deviation 0.10, relative error 1.1%, skewness −0.02, kurtosis −0.05.
[c] Result for initial chemical composition.
[d] Average of results of all 20,000 trials.

The trials that are devoid of significant majorite content (<0.4 mol%) exhibit a Gaussian distribution for pyrope (cf. footnote of Table 6).

The magnification of error can be observed by comparing the relative error of the input concentrations with the relative error of the output proportions in Table 6, and may be understood in a qualitative sense as a result of the distribution of elements among more than one structural site, more than one valence state, and among more than one end-member. Thus, the distribution of Ca among four end-members, and the calculation by stoichiometry of Fe^{3+} and Fe^{2+}, lead to higher relative uncertainty for andradite, grossular and almandine then is observed for spessartine (Table 6). As a rule, the abundance of end-members is negatively correlated in a rough fashion with their uncertainty, i.e., minor end-members will tend to have high uncertainty, and this tendency should be taken into consideration by any user of this spreadsheet. In addition, the minor components may not exhibit truly Gaussian distributions because their proportions have been rounded to two decimal places.

6. System requirements and program availability

In order to make use of the spreadsheet, Microsoft Excel must be installed on the computer, which should have at least 256 MB RAM, and a Pentium III-equivalent (or faster, preferably much faster) processor, because of the size of the spreadsheet. This large spreadsheet (~12 MB) is available from www.iamg.org as an electronic deposit item in the form of a compressed file (~3 MB), or from the author.

Acknowledgments

The encouragement and comments on the manuscript of T. Chacko and R.W. Luth are gratefully acknowledged, and thanks are extended to T. Stachel for several literature references. The careful reviews of referees A.R. Chakhmouradian and T. Theye helped improve this paper.

Appendix A. Supporting Information

Supplementary data associated with this article can be found in the online version at doi:10.1016/j.cageo.2007.12.013.

References

Amthauer, G., Rossman, G.R., 1998. The hydrous component in andradite garnet. American Mineralogist 83, 835–840.

Amthauer, G., McIver, J.R., Viljoen, E.A., 1979. ^{57}Fe and ^{119}Sn Mössbauer studies of natural tin-bearing garnets. Physics and Chemistry of Minerals 4, 235–244.

Armbruster, T., Birrer, J., Libowitzky, E., Beran, A., 1998. Crystal chemistry of Ti-bearing andradites. European Journal of Mineralogy 10, 907–921.

Armbruster, T., Kohler, T., Libowitzky, E., Friedrich, A., Miletich, A., Kunz, M., Medenbach, O., Gutzmer, J., 2001. Structure, compressibility, hydrogen bonding, and dehydration of the tetragonal Mn^{3+} hydrogarnet, henritermierite. American Mineralogist 86, 147–158.

Atuchin, V.V., Kesler, V.G., Pervukhina, N.V., Zhang, Z., 2006. Ti 2p and O 1s core levels and chemical bonding in titanium-bearing oxides. Journal of Electron Spectroscopy and Related Phenomena 152, 18–24.

Basso, R., 1987. The crystal structure of palenzonaite, a new vanadate garnet from Val Graveglia (Northern Apennines, Italy). Neues Jahrbuch für Mineralogie-Monatshefte, 136–144.

Berger, A., Scherrer, N.C., Bussy, F., 2005. Equilibration and disequilibration between monazite and garnet: indication from phase-composition and quantitative texture analysis. Journal of Metamorphic Geology 23, 865–880.

Boctor, N.Z., Bell, P.M., Mao, H.K., Kullerud, G., 1982. Petrology and shock metamorphism of Pampa del Infierno chondrite. Geochimica et Cosmochimica Acta 46, 1903–1911.

Bubeck, W., Machatschki, F., 1935. Die Kristallstruktur des Berzeliit $(Ca,Na)_3(Mg,Mn)_2(AsO_4)_3$ (The crystal structure of berzeliite $(Ca,Na)_3(Mg,Mn)_2(AsO_4)_3$). Zeitschrift für Kristallographie 90, 44–50.

Bühn, B., Okrusch, M., Woermann, E., Lehnert, K., Hoernes, S., 1995. Metamorphic evolution of Neoproterozoic manganese formations and their country rocks at Otjosondu, Namibia. Journal of Petrology 36, 463–496.

Burt, D.M., 1991. Vectors, components, and minerals. American Mineralogist 76, 1033–1037.

Carley, A.F., Chalker, P.R., Rivieret, J.C., Roberts, M.W., 1987. The identification and characterisation of mixed oxidation states at oxidised titanium surfaces by analysis of X-ray photoelectron spectra. Journal of the Chemical Society—Faraday Transactions 83, 351–370.

Cenki-Tok, B., Chopin, C., 2006. Coexisting calderite and spessartine garnets in eclogite-facies metacherts of the Western Alps. Mineralogy and Petrology 88, 47–68.

Chakhmouradian, A.R., McCammon, C.A., 2005. Schorlomite: a discussion of the crystal chemistry, formula, and inter-species boundaries. Physics and Chemistry of Minerals 32, 277–289.

Chakhmouradian, A.R., Cooper, M.A., Medici, L., Hawthorne, F.C., Adar, F., 2008. Fluorine-rich hibschite from silicocarbonatite, Afrikanda (Russia): crystal chemistry and crystallization conditions. Canadian Mineralogist 46, in press.

de Groot, F.M.F., Figueiredo, M.O., Basto, M.J., Abbate, M., Petersen, H., Fuggle, J.C., 1992. 2*p* X-ray absorption of titanium in minerals. Physics and Chemistry of Minerals 19, 140–147.

Deer, W.A., Howie, R.A., Zussman, J., 1997. Orthosilicates, second ed. Volume 1A, Rock-Forming Minerals. The Geological Society, London, UK, 919pp.

Droop, G.T.R., 1987. A general equation for estimating Fe^{3+} concentrations in ferromagnesian silicates and oxides from microprobe analyses using stoichiometric criteria. Mineralogical Magazine 51, 431–435.

Dwarzski, R.E., Draper, D.S., Shearer, C.K., Agee, C.B., 2006. Experimental insights on crystal chemistry of high-Ti garnets from garnet-melt partitioning of rare-earth and high-field-strength elements. American Mineralogist 91, 1536–1546.

Enami, M., Cong, B., Yoshida, T., Kawabe, I., 1995. A mechanism for Na incorporation in garnet: an example from garnet in orthogneiss from the Su–Lu terrane, eastern China. American Mineralogist 80, 475–482.

Farges, F., Brown Jr., G.E., Rehr, J.J., 1997. Ti *K*-edge XANES studies of Ti coordination and disorder in oxide compounds: comparison between theory and experiment. Physical Review B 56, 1809–1819.

Ferro, O., Galli, E., Papp, G., Quartieri, S., Szakáll, S., Vezzalini, G., 2003. A new occurrence of katoite and re-examination of the hydrogrossular group. European Journal of Mineralogy 15, 419–426.

Flohr, M.J.K., Ross, M., 1989. Alkaline igneous rocks of Magnet Cove, Arkansas: metasomatized ijolite xenoliths from Diamond Jo quarry. American Mineralogist 74, 113–131.

Friberg, L.M., 1989. Garnet stoichiometry program using a Lotus 1-2-3 spreadsheet. Computers & Geosciences 15, 1169–1172.

Frost, B.R., 1991. Introduction to oxygen fugacity and its petrologic importance. Reviews in Mineralogy 25, 1–9.

Galuskina, I.O., Galuskin, E.V., Dzierzanowski, P., Armbruster, T., Kozanecki, M., 2005. A natural Scandian garnet. American Mineralogist 90, 1688–1692.

Geiger, C.A., 2004. Spectroscopic investigations relating to the structural, crystal-chemical and lattice-dynamic properties of $(Fe^{2+},Mn^{2+},Mg,Ca)_3Al_2Si_3O_{12}$ garnet: a review and analysis. In: Beran, A., Libowitzky, E. (Eds.), Spectroscopic Methods in Mineralogy. EMU Notes in Mineralogy, vol. 6. Eötvös University Press, Budapest, pp. 589–645.

Geiger, C.A., Armbruster, T., 1997. $Mn_3Al_2Si_3O_{12}$ spessartine and $Ca_3Al_2Si_3O_{12}$ grossular garnet: structural dynamic and thermodynamic properties. American Mineralogist 82, 740–747.

Geiger, C.A., Stahl, A., Rossman, G.R., 2000. Single-crystal IR- and UV/VIS-spectroscopic measurements on transition metal bearing pyrope: the incorporation of hydroxide in garnet. European Journal of Mineralogy 12, 259–271.

Geller, S., 1967. Crystal chemistry of the garnets. Zeitschrift für Kristallographie 125, 1–47.

Giaramita, M.J., Day, H.W., 1990. Error propagation in calculations of structural formulas. American Mineralogist 75, 170–182.

Hålenius, U., 2004. Stabilization of trivalent Mn in natural hydrogarnets on the join 'hydrogrossular'–henritermierite, $Ca_3Mn_2^{3+}[SiO_4]_2[H_4O_4]$. Mineralogical Magazine 68, 335–341.

Hålenius, U., Häussermann, U., Harryson, H., 2005. Holtstamite, $Ca_3(Al,Mn^{3+})_2(SiO_4)_{3-x}(H_4O_4)_x$, a new tetragonal hydrogarnet from Wessels Mine, South Africa. European Journal of Mineralogy 17, 375–382.

Hawthorne, F.C., 1981. Some systematics of the garnet structure. Journal of Solid State Chemistry 37, 157–164.

Hawthorne, F.C., 2002. The use of end-member charge-arrangements in defining new mineral species and heterovalent substitutions in complex minerals. Canadian Mineralogist 40, 699–710.

Henmi, C., Kusachi, I., Henmi, K., 1995. Morimotoite, $Ca_3TiFe^{2+}Si_3O_{12}$, a new titanian garnet from Fuka, Okayama Prefecture, Japan. Mineralogical Magazine 59, 115–120.

Ihinger, P.D., Stolper, E.M., 1986. The color of meteoritic hibonite: an indicator of oxygen fugacity. Earth and Planetary Science Letters 78, 68–79.

Ito, J., 1968. Synthesis of the berzeliite ($Ca_2NaMg_2As_3O_{12}$)-manganese berzeliite ($Ca_2NaMn_2As_3O_{12}$) series (arsenate garnet). American Mineralogist 53, 316–319.

Jarosch, D., Zemann, J., 1989. Yafsoanite: a garnet type calcium-tellurium(VI)-zinc oxide. Mineralogy and Petrology 40, 111–116.

Kingma, K.J., Downs, J.W., 1989. Crystal-structure analysis of a birefringent andradite. American Mineralogist 74, 1307–1316.

Knowles, C.R., 1987. A BASIC program to recast garnet end-members. Computers & Geosciences 13, 655–658.

Krause, W., Blass, G., Effenberger, H., 1999. Schäferite, a new vanadium garnet from the Bellberg volcano, Eifel, Germany. Neues Jahrbuch für Mineralogie, Monatshefte, 123–134.

Labotka, T.C., 1995. Evidence for immiscibility in Ti-rich garnet in a calc-silicate hornfels from northeastern Minnesota. American Mineralogist 80, 1026–1030.

Lager, G.A., Armbruster, T., Rotella, F.J., Rossman, G.R., 1989. OH substitution in garnets: X-ray and neutron diffraction, infrared, and geometric-modeling studies. American Mineralogist 74, 840–851.

Libowitzky, E., Beran, A., 2004. IR spectroscopic characterization of hydrous species in minerals. In: Beran, A., Libowitzky, E. (Eds.), Spectroscopic Methods in Mineralogy. EMU Notes in Mineralogy, vol. 6. Eötvös University Press, Budapest, pp. 227–279.

Locock, A., Luth, R.W., Cavell, R.G., Smith, D.G.W., Duke, M.J.M., 1995. Spectroscopy of the cation distribution in the schorlomite species of garnet. American Mineralogist 80, 27–38.

Luth, R.W., Virgo, D., Boyd, F.R., Wood, B.J., 1990. Ferric iron in mantle-derived garnets: implications for thermobarometry and for the oxidation state of the mantle. Contributions to Mineralogy and Petrology 104, 56–72.

Malitesta, C., Losito, L., Scordari, F., Schingaro, E., 1995. XPS investigation of titanium in melanites from Monte Vulture (Italy). European Journal of Mineralogy 7, 847–858.

Mandarino, J.A., 1981. The Gladstone–Dale relationship. IV. The compatibility concept and its application. Canadian Mineralogist 19, 441–450.

Mandarino, J.A., Back, M.E., 2004. Fleischer's Glossary of Mineral Species 2004. The Mineralogical Record Inc., Tucson, AZ, 310pp.

Menzer, G., 1927. Die Kristallstruktur von Kryolithionit (The crystal structure of cryolithionite). Zeitschrift für Kristallographie 66, 457–458.

Muhling, J.R., Griffin, B.J., 1991. On recasting garnet analyses into end-member molecules—revisited. Computers & Geosciences 17, 161–170.

Nickel, E.H., Grice, J.D., 1998. The IMA commission on new minerals and mineral names: procedures and guidelines on mineral nomenclature, 1998. Canadian Mineralogist 36, 913–926.

Novak, G.A., Gibbs, G.V., 1971. The crystal chemistry of the silicate garnets. American Mineralogist 56, 791–825.

Oberti, R., Quartieri, S., Dalconi, M.C., Boscherini, F., Iezzi, G., Boiocchi, M., Eeckhout, S.G., 2006. Site preference and local geometry of Sc in garnets: Part I. Multifarious mechanisms in the pyrope–grossular join. American Mineralogist 91, 1230–1239.

Pertlik, F., 2003. Bibliography of hibschite, a hydrogarnet of grossular type. GeoLines 15, 113–119.

Platt, R.G., Mitchell, R.H., 1979. The Marathon Dikes. I: zirconium-rich titanian garnets and manganoan magnesian ulvöspinel-magnetite spinels. American Mineralogist 64, 546–550.

Quartieri, S., Boscherini, F., Chaboy, J., Dalconi, M.C., Oberti, R., Zanetti, A., 2002. Characterization of trace Nd and Ce site preference and coordination in natural melanites: a combined X-ray diffraction and high-energy XAFS study. Physics and Chemistry of Minerals 29, 495–502.

Quartieri, S., Oberti, R., Boiocchi, M., Dalconi, M.C., Boscherini, F., Safonova, O., Woodland, A.B., 2006. Site preference and local geometry of Sc in garnets: Part II. The crystal-chemistry of octahedral Sc in the andradite–$Ca_3Sc_2Si_3O_{12}$ join. American Mineralogist 91, 1240–1248.

Rager, H., Geiger, C.A., Stahl, A., 2003. Ti(III) in synthetic pyrope: a single-crystal electron paramagnetic resonance study. European Journal of Mineralogy 15, 697–699.

Rickwood, P.C., 1968. On recasting analyses of garnet into end-member molecules. Contributions to Mineralogy and Petrology 18, 175–198.

Schingaro, E., Scordari, F., Pedrazzi, G., Malitesta, C., 2004. Ti and Fe speciation by X-ray photoelectron spectroscopy (XPS) and Mössbauer spectroscopy for a full chemical characterization of Ti-garnets from Colli Albani (Italy). Annali di Chimica 94, 185–196.

Seifert, A.V., Vrána, S., 2005. Bohemian garnet. Bulletin of Geosciences 80, 113–124.

Smith, J.V., Mason, B., 1970. Pyroxene-garnet transformation in Coorara meteorite. Science 168, 832–833.

Smyth, J.R., Madel, R.E., McCormick, T.C., Munoz, J.L., Rossman, G.R., 1990. Crystal-structure refinement of a fluorine-bearing spessartine garnet. American Mineralogist 75, 314–318.

Spear, F.S., 1993. The calculation of metamorphic phase equilibria I: geothermometry and geobarometry. In: Metamorphic Phase Equilibria and Pressure–Temperature–Time Paths. Mineralogical Society of America, Washington, DC, pp. 511–545.

Stachel, T., 2001. Diamonds from the aesthenosphere and the transition zone. European Journal of Mineralogy 13, 883–892.

Stachel, T., Banas, A., Muehlenbachs, K., Kurszlaukis, S., Walker, E.C., 2006. Archean diamonds from Wawa (Canada): samples from deep cratonic roots predating cratonization of the Superior Province. Contributions to Mineralogy and Petrology 151, 737–750.

Tappert, R., Stachel, T., Harris, J.W., Muehlenbachs, K., Ludwig, T., Brey, G.P., 2005. Diamonds from Jagersfontein (South Africa): messengers from the sublithospheric mantle. Contributions to Mineralogy and Petrology 150, 505–522.

Uher, P., Chovan, M., Majzlan, J., 1994. Vanadian–chromian garnet in mafic pyroclastic rocks of the Malé Karpaty Mountains, western Carpathians, Slovakia. Canadian Mineralogist 32, 319–326.

Virgo, D., Rosenhauer, M., Huggins, F.E., 1976. Intrinsic oxygen fugacities of natural melanites and schorlomites and crystal-chemical implications. Carnegie Institution of Washington Yearbook 75, 720–729.

Virgo, D., Luth, R.W., Moats, M.A., Ulmer, G.C., 1988. Constraints on the oxidation state of the mantle: an electrochemical and ^{57}Fe Mössbauer study of mantle-derived ilmenites. Geochimica et Cosmochimica Acta 52, 1781–1794.

Waychunas, G.A., 1986. Examination of Ti XANES spectra of minerals and solids: effects of site geometry on spectral features. Journal de Physique, Colloque C8 47, C8-841–C8-844.

Waychunas, G.A., 1987. Synchrotron radiation XANES spectroscopy of Ti in minerals: effects of Ti bonding distances, Ti valence, and site geometry on absorption edge structure. American Mineralogist 72, 89–101.

Yang, J., 1991. A new scheme for calculating mineral end-members with reference to clinopyroxene and garnet. Acta Geologica Sinica 65, 360–366.